Available online at www.sciencedirect.com
ScienceDirect
Trans. Nonferrous Met. Soc. China 24(2014) 1730−1736
Transactions of Nonferrous Metals Society of China
www.tnmsc.cn

Effect of carbon on microstructures of Ti−45Al−3Fe−2Mo−*x*C alloy

Can-xu ZHOU, Bin LIU, Yong LIU, Cong-zhang QIU, Yue-hui HE

State Key Laboratory of Powder Metallurgy, Central South University, Changsha 410083, China

Received 8 July 2013; accepted 3 December 2013

Abstract: The effect of carbon addition on the microstructures of TiAl-based alloy (Ti−45Al−3Fe−2Mo) was studied. The proportion of $\beta/B2$ phase reduces with the content of carbon increasing, while the colony size increases. With increasing the carbon content, the lamellar spacing first decreases from 267 nm (Ti−45Al−3Fe−2Mo) to 237 nm (Ti−45Al−3Fe−2Mo−0.3C) and 155 nm (Ti−45Al−3Fe−2Mo−0.5C), but then increases to 230 nm (Ti−45Al−3Fe−2Mo−1.0C) with further increase in C level, which is affected by the inhibition of carbon atom and precipitation of carbides at the lamellar interface. Precipitation of carbides shows a response to aging time at 800 °C. P-type carbides grow up at the boundaries and near the dislocation areas with the prolonging of aging time. And these carbides are projected different morphology in different beam directions (BD). The effects of these microstructural modifications were examined and the observations were discussed.

Key words: TiAl alloy; carbon doping; microstructure; carbide

1 Introduction

Gamma-TiAl alloys are potential candidates for high-temperature structure aero-space application because of their low density and superior high-temperature properties [1,2]. However, the low ductility and poor formability restrict their applications [3,4]. Lots of investigations have been conducted on how to enhance the ductility and hot workability of gamma-TiAl by alloying with elements [5], heat-treatment or thermo-mechanical deformation [6,7], which are essential for microstructure modifications and property improvement of TiAl alloys.

Recently, in order to improve the low temperature deformability, the TiAl alloy has been developed by adding Fe, Mo elements. QIU et al [8,9] found that the Ti−45Al−3Fe−2Mo alloy (β-TiAl) has full-colony microstructure with β and γ phases coexisting along the grain boundaries. This alloy shows an outstanding high-temperature deformability, which is related with the dynamic recrystallization occurring in β grains at elevated temperatures. As a consequence, Ti−45Al−3Fe−2Mo exhibits a high deformability above 750 °C, and a superplastic behavior at 790 °C. However, superplasticity is achieved at the cost of the decline of creep properties. The coarse β phase along the grain boundary and lamellar interfaces degrades the creep resistance [10]. Many researches have shown that interstitial elements such as C, N, O contained in TiAl alloys as addition can improve the creep resistance of TiAl alloy [11−15]. PARK et al [16] reported that the addition of interstitial elements is instrumental in producing a significant refinement in colony size and lamellar spacing, which can improve the creep resistance. Furthermore, in the γ phase, where the solubility of C is low, precipitates form at low interstitial concentration areas, leading to strong interactions between impurities, precipitates and dislocations [17].

The addition of C in TiAl can form two kinds of precipitates during different thermal treatment and aging conditions, which have already been noted in Refs. [12,14−19]. The precipitates are identified as needle-like Ti_3AlC (aged at 1073 K) with the perovskite structure and plate-like Ti_2AlC (aged at 1523 K) with an *H*-phase structure. These formations of precipitates can not only refine the colony size and lamellar thickness, but also increase the strength by age-hardening. During the deformation process, the dislocations are effectively pinned by these precipitates.

Several studies showed the beneficial effect of carbon on solid-solution hardening and precipitation

Foundation item: Project (2011CB605505) supported by the National Basic Research Program of China
Corresponding author: Yong LIU; Tel: +86-731-88836939; E-mail: yonliu@csu.edu.cn
DOI: 10.1016/S1003-6326(14)63246-5

strengthening in γ-TiAl [15−19]. But few work studied the effect of carbon on the microstructure of β-TiAl. This study aims to investigating the role of carbon in the microstructure of β phase-containing TiAl, and developing a TiAl alloy not only possessing a sound deformability, but also presenting good creep resistance. This will be significant to improving the application of β-TiAl. Reasons for the observed changes in microstructure are discussed.

2 Experimental

The nominal composition of TiAl alloys was Ti−45Al−3Fe−2Mo. Several levels of carbon, 0.3%, 0.5%, 1.0% in mole fraction, were incorporated into the base alloy. Alloys were prepared using a vacuum arc-melting furnace and each was remelted four times to ensure compositional homogeneity. The ingot was subjected to a homogenization heat treatment, (1170 °C, 20 h)+(1250 °C, 1 h)+furnace cooling, and then heat treated at 1310 °C for 15 min. Finally, the aging treatments at 800 °C for 4 h, 15 h, 36 h and 75 h followed by furnace cooling to room temperature were performed to precipitate fine carbides.

The transformation characteristics were examined by differential thermal analysis (DTA). The microstructure was characterized by scanning electron microscopy (SEM, FEI Nova SEM 230) and transmission electron microscopy (TEM JOEL 2100). The thin foils for TEM observation were prepared by electropolishing using a twin-jet polisher in electrolyte solution containing 5% perchloric acid, 35% *n*-butanol and 60% methanol (volume fraction) at −30 °C and 21 V. The chemical compositions of the alloys were tested by EPMA.

3 Results and discussion

3.1 DTA curves of Ti−45Al−3Fe−2Mo−*x*C

Figure 1 shows the DTA curves of Ti−45Al−3Fe−2Mo and Ti−45Al−3Fe−2Mo−*x*C alloys with several endothermic peaks, upon heating from 900 °C to 1500 °C. The first endothermic peak has an onset at about 1260 °C for all the alloys, which is associated with α transus (T_α). With increasing temperature, the second endothermic peak has an onset at 1500 °C for Ti−45Al−3Fe−2Mo−0.5C and Ti−45Al−3Fe−2Mo−1.0C alloys. This is associated with a phase transformation from α phase to β phase (T_β). The features of Ti−45Al−3Fe−2Mo−0.5C and Ti−45Al−3Fe−2Mo−1.0C alloys are almost similar. The T_α values of these two alloys are 1257 °C and 1254 °C respectively, and the T_β values tend to be similar, nearly 1476 °C. High-temperature β phase contains many β phase stabilizer elements, resulting in a fact that the diffusion transformation β/α cannot proceed completely at a rather quick cooling rate [20]. Therefore, Ti−45Al−3Fe−2Mo and Ti−45Al−3Fe−2Mo−0.3C alloys do not show the T_β peak obviously, and the T_α is nearly the same, which is 1260 °C. It can be concluded from Fig. 1 that the addition of carbon can widen the α phase field.

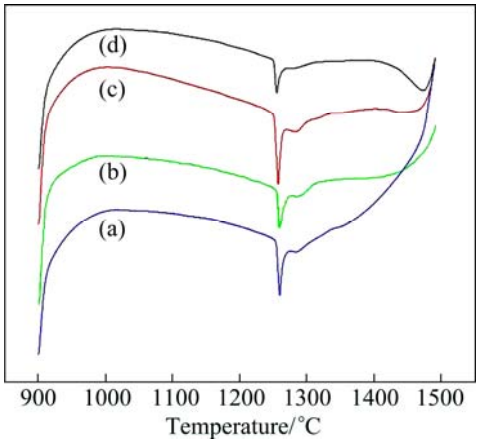

Fig. 1 DTA curves of Ti−45Al−3Fe−2Mo alloys with different carbon content: (a) Ti−45Al−3Fe−2Mo; (b) Ti−45Al−3Fe−2Mo−0.3C; (c) Ti−45Al−3Fe−2Mo−0.5C; (d) Ti−45Al−3Fe−2Mo−1.0C

3.2 Microstructures

Figure 2 shows the SEM images of the Ti−45Al−3Fe−2Mo ingots with various C contents. Ti−45Al−3Fe−2Mo ingot exhibits the structure with fine γ and $\beta/B2$ ($B2$ phase is low-temperature ordered β phase) along the lamellar colonies. The white phase is $\beta/B2$ phase, and the dark phase is γ phase. When carbon content increases to 0.3%, the phase constitution is similar to C free alloy, but some larger lamellar colonies can be observed at the same magnification. When further increasing the content of C to 0.5% and 1.0%, these two alloys have a near full lamellar structure.

After being heat-treated at 1310 °C for 15 min, colony size rapidly increases with increasing carbon content in the alloys as shown in Fig. 3, and the proportion of β phase decreases obviously with the increase of carbon. The average colony sizes and the content of β phase for these alloys are provided in Table 1.

The microstructure was also observed by TEM. The mean lamellar spacing is shown in Table 1. Compared with Ti−45Al−3Fe−2Mo, the addition of 0.3% C can refine the lamellar spacing and increase the thickness of α_2 lath (Figs. 4(a) and (b)). A careful examination of the lamellar interfaces as well as the lamellar inferior reveals no obvious precipitates. The microstructure of the alloy containing 0.5% carbon shows a fine and uniform lamellar structure (Fig. 4(c)). The lamellar spacing on an

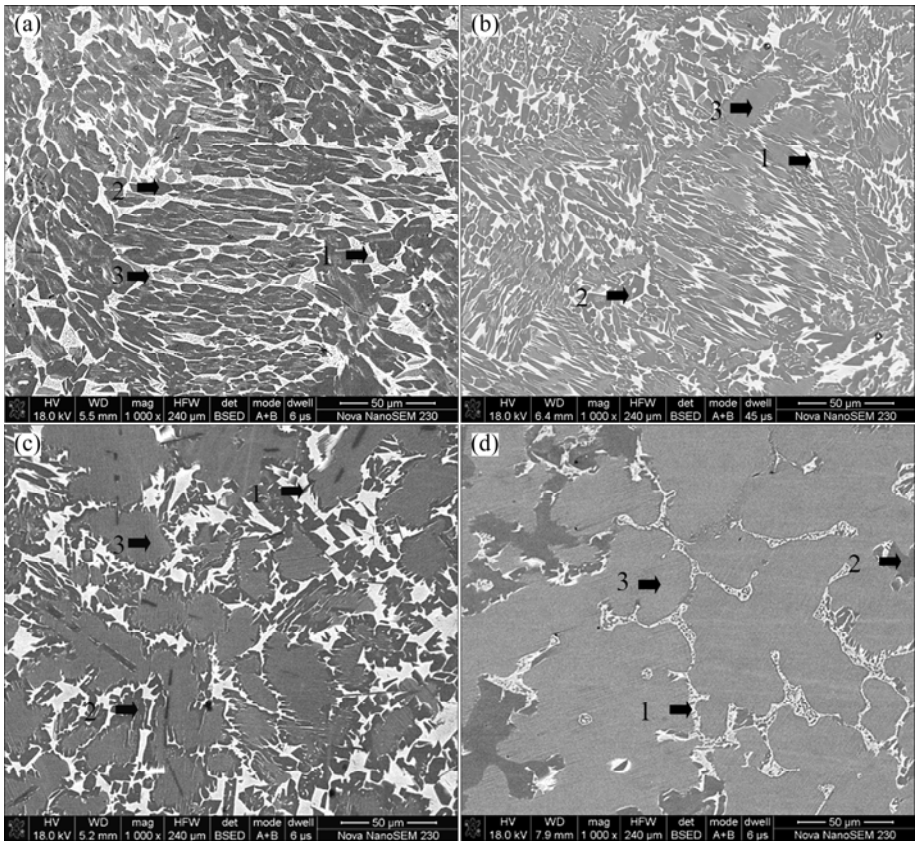

Fig. 2 SEM images of as-cast Ti−45Al−3Fe−2Mo ingots with various C contents: (a) Ti−45Al−3Fe−2Mo; (b) Ti−45Al−3Fe−2Mo−0.3C; (c) Ti−45Al−3Fe−2Mo−0.5C; (d) Ti−45Al−3Fe−2Mo−1.0C (1—*β*/*B*2 phase; 2—*γ* phase; 3—Lamellar colony)

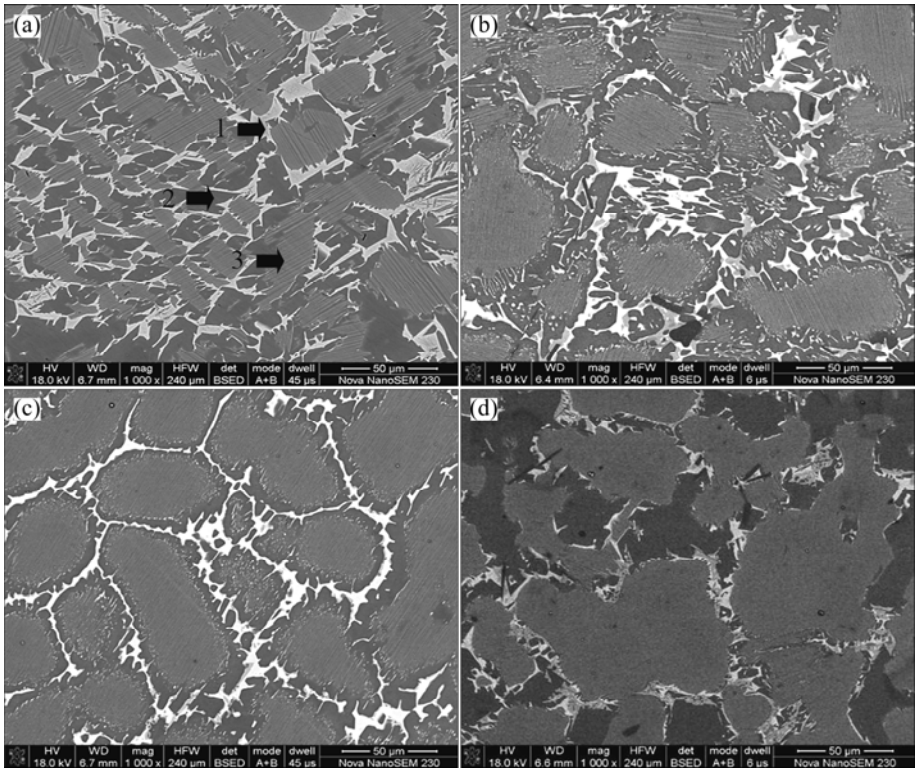

Fig. 3 SEM images of Ti−45Al−3Fe−2Mo ingots after 1300 °C heat-treatment: (a) Ti−45Al−3Fe−2Mo; (b) Ti−45Al−3Fe−2Mo−0.3C; (c) Ti−45Al−3Fe−2Mo−0.5C; (d) Ti−45Al−3Fe−2Mo−1.0C (1—*β*/*B*2 phase; 2—*γ* phase; 3—Lamellar colony)

Table 1 Size of colonies, proportion of β phase and lamellar spacing in various carbon-containing alloys

Alloy	Size of colony/μm	Proportion of β phase/%	Lamellar spacing/nm
Ti−45Al−3Fe−2Mo	24.2	15.4	267
Ti−45Al−3Fe−2Mo−0.3C	42.1	11.5	237
Ti−45Al−3Fe−2Mo−0.5C	52.6	9.7	155
Ti−45Al−3Fe−2Mo−1.0C	78.6	6.8	230

average is further decreased to 155 nm. While in the alloy containing 1.0% carbon, the lamellar spacing is increased to 230 nm, and the lamellar microstructure contains coarse precipitates (Fig. 5(a)). Figures 5(b) and (d) show the HREM image and corresponding FFT images of carbide in the α_2/γ interface, with the incident electron beam parallel to $[110]_\gamma$. Carbides grow at the expense of the α_2 lath and lead to the precipitation of $\beta/B2$ phase shown in Figs. 5(a) and (c).

The effect of carbon on the microstructure of Ti−45Al−3Fe−2Mo can be summarized as follows. 1) The proportion of $\beta/B2$ phase decreases substantially with increasing carbon level. 2) The average colony size increases with increasing carbon content. 3) The mean lamellar thickness first decreases with 0.3% and 0.5% carbon addition but then increases with further increase of carbon. 4) Carbides can be formed at the boundaries or along dislocation lines in Ti−45−Al−3Fe−2Mo alloy. Carbon is an α-stabilizing element, and it can reduce the amount of retained $\beta/B2$ particles and inevitably influence the effect of $\beta/B2$ phase on decreasing the colonies size. Carbon can also refine the lamellar spacing [17], but excess carbon can make an opposite effect.

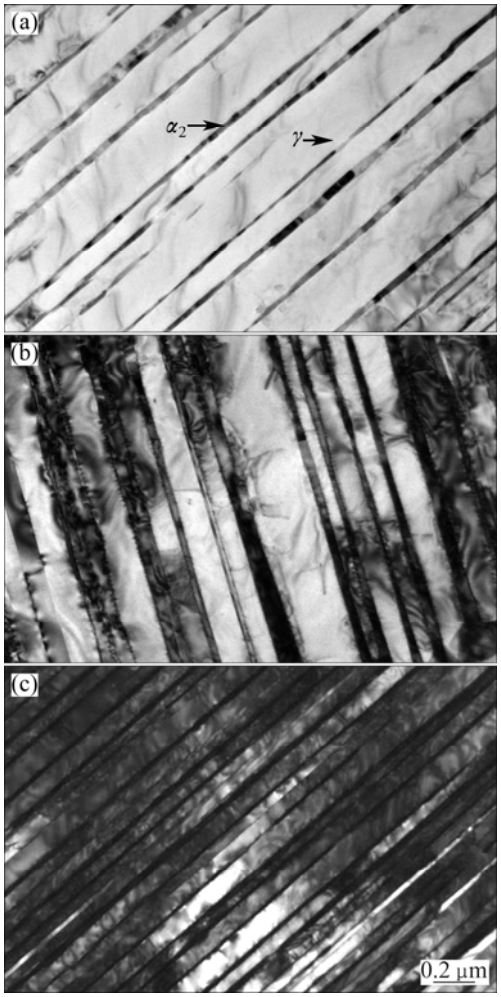

Fig. 4 TEM images of lamellar structure of alloys: (a) Ti−45Al−3Fe−2Mo; (b) Ti−45Al−3Fe−2Mo−0.3C; (c) Ti−45Al−3Fe−2Mo−0.5C

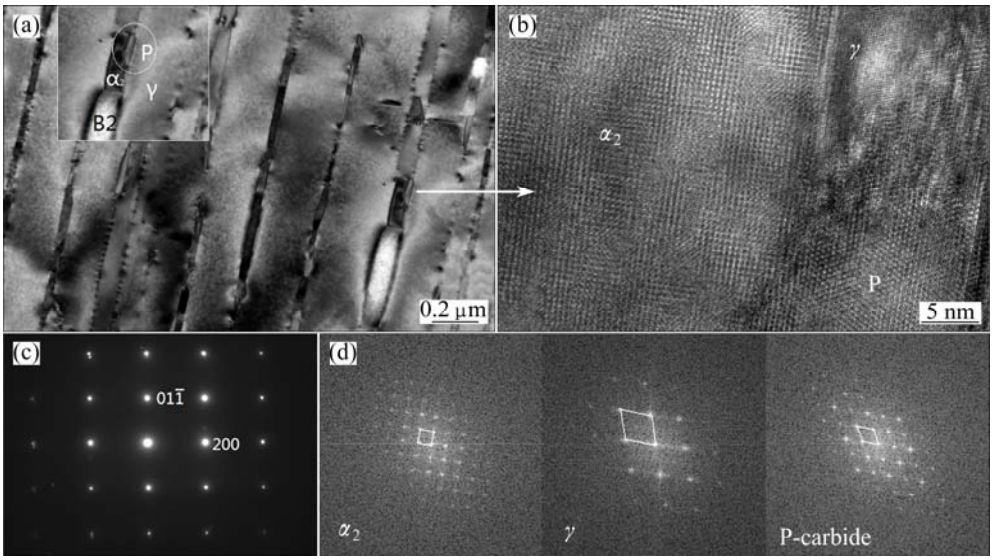

Fig. 5 TEM image of lamellar structure of Ti−45Al−3Fe−2Mo−1.0C (a), HREM image of carbides (P−carbide Ti_3AlC) precipitated at interface of lamellar (b), SAED pattern of $B2$ phase precipitated from lamellar area (c), and corresponding FFT images of (b) with $(0001)\alpha_2//(111)_\gamma//(111)_P$, $[11\bar{2}0]\alpha_2//[\bar{1}01]_\gamma$ (d)

During the transformation from α to α_2/γ, the longitudinal and lateral growth of the lamellar precipitates occurs through the "terrace-ledge-kink" mechanism, the transferring of atoms onto kinks which provide favorable sites to the atomic attachment. The growth of the lamellar γ phase slows down and can stop with a gradually decreasing solute supersaturation in the matrix, reducing the driving force for the ledge movement [21]. Carbon addition can affect the composition change during the lamellar structure formation process and the carbon atom can hinder the transfer of atoms onto kinks, so decreasing the rate of nucleation and lateral thickening of the γ lamellae plates. Therefore, carbon can refine the lamellar spacing. While compared with alloy with 0.5%C, the mean lamellar spacing in the alloy with 1.0% C is increased. Figure 6(a) exhibits that more addition of C can result in more carbides (Ti_3AlC) precipitating along the lamellar interface, which can change the Al concentration in the TiAl matrix. The formation of carbides will strip the Ti from the matrix and render more Al rich. And the alloy with higher Al concentration had a coarser mean lamellar thickness. So, there is a coarser lamellar spacing in the alloy with 1.0%C.

3.3 Existence of carbides

The content of carbon in different phases was measured by EMPA, and the results are presented in Table 2. It can be seen that less interstitial carbon is dissolved in γ, whereas the lamellar colonies have a high content of carbon.

Table 2 Distribution of C in different phases of Ti−45Al−3Fe−2Mo

Alloy	Carbon content/%		
	Lamellar	γ phase	$B2$ phase
Ti−45Al−3Fe−2Mo−0.3C	0.52	0.07	0.19
Ti−45Al−3Fe−2Mo −0.5C	0.64	0.11	0.23
Ti−45Al−3Fe−2Mo −1.0C	0.70	0.13	0.22

According to the Ti−Al−C phase diagram, at 900−1310 °C, two types of carbides exist in the composition range of (15%−55%)Al and (0.1%−1.0%)C, which are Ti_3AlC and Ti_2AlC. Usually, the needle-like precipitate Ti_3AlC is of perovskite type, which precipitates at 800 °C, and at a higher temperature or for longer aging time, the plates-like precipitates Ti_2AlC are formed. Besides precipitating at the boundaries and lamellar interface, fine dispersions of Ti_3AlC perovskite precipitates can form arrays along the dislocation lines, and can provide a significant influence for improving the mechanical performance at elevated temperatures. In comparison, carbon in solid solution or in the form of coarse Ti_2AlC particles is less efficient for hardening the material [4].

Figures 6(a) and (b) show the precipitates in the alloy containing 0.5% C aged at 800 °C for 4 h. Few precipitate is found at the boundary or near the dislocation lines. And more precipitates are found with prolonging aging time to 15 h, as shown in Figs. 6(c) and (d). Figure 7 shows the precipitates in the alloy with

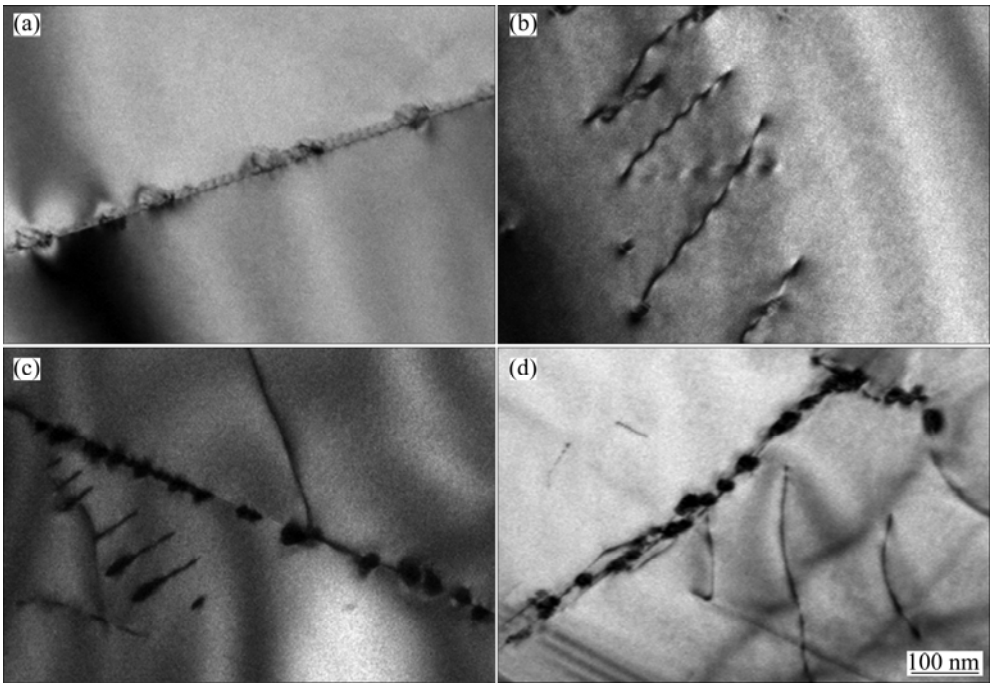

Fig. 6 Bright-field TEM image of Ti−45Al−3Fe−2Mo−0.5C alloys aged at 800 °C for 4 h (a,b) and 15 h (c,d): (a, c) Boundaries area; (b, d) Dislocations areas

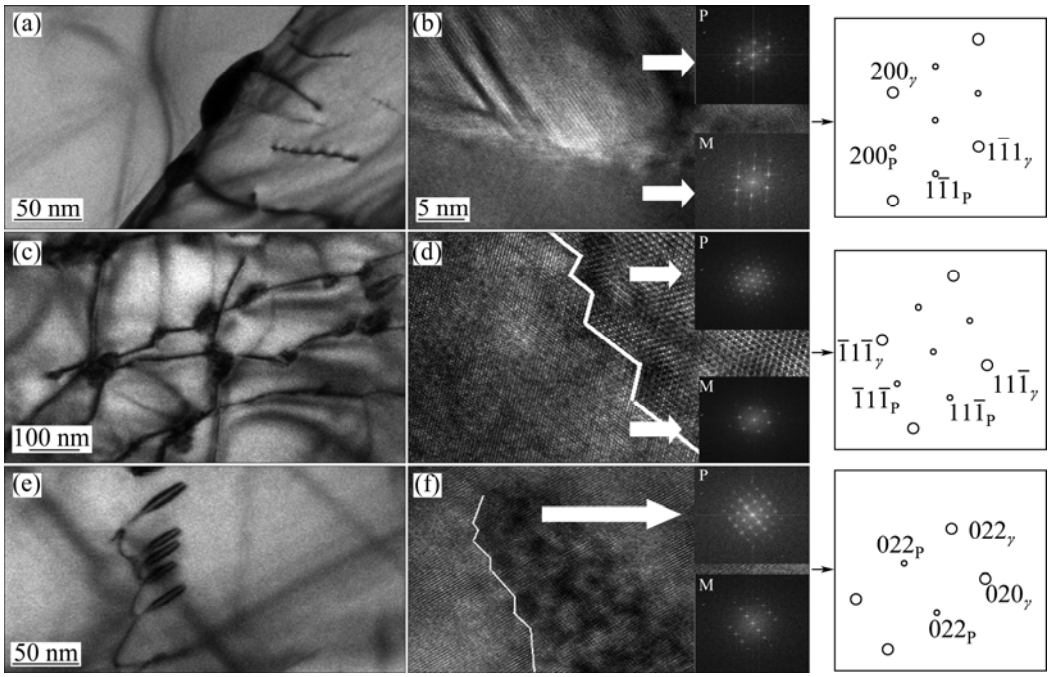

Fig. 7 TEM images of alloy with 0.5% C aged at 800 °C for 36 h showing Ti_3AlC precipitates formed at boundaries (a) and dislocations (c, e), HREM image showing carbide formed at boundary (BD=[011]) (b) and near dislocation areas (BD=[011]) (d), (BD=[100]) (f) (P is Ti_3AlC; M is matrix)

0.5% C aged at 800 °C for 36 h. Precipitates at the boundary or near the dislocation lines grow up. Figures 7(b, d, f) show HREM images of these precipitates. These precipitates have a perovskite structure, Ti_3AlC, which has the orientation relationship to γ of $(001)_P//(001)_{TiAl}$ and $[010]_P//[010]_{TiAl}$. When the precipitates are imaged from the [100] direction of the TiAl matrix, they are projected as needle shape, while from the [110] direction, the precipitates show a round shape. All these precipitates can pin the dislocations and improve the strength.

More and coarser precipitates are found after extending aging time to 75 h. The needle-like precipitates grow up to longer than 400 nm, as shown in Fig. 8(a). And as these coarse carbides precipitated, some other precipitates are found in the matrix, and the corresponding SAED patterns exhibit that these fine precipitates are β/B_2 phase (Fig. 8(b)).

Dislocations offer the nucleation position for precipitations while these precipitates can affect the dislocation motion and result in the strengthening effect. A significant feature of the image is that, near the dislocation areas, the interface between the carbide and γ phase is not flat but is composed of a few ledges. It may suggest that the interaction between the diffusive solute atoms and the moving dislocation dominates the formation process of the carbides. In the γ-matrix, carbon-rich zone provides the necessary condition for carbide nucleation, and dislocations can also provide nucleation sites of the carbides. As the aging time prolonged, the possibility of the interaction between the carbon-rich zone and dislocation was increased, which increased the size and the number of carbides.

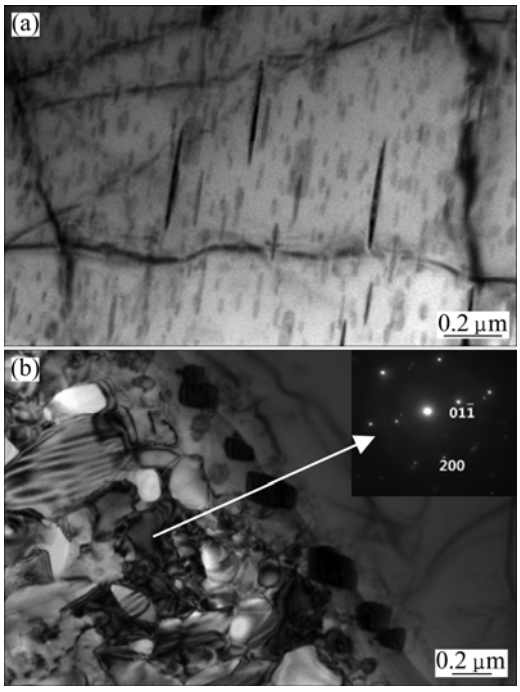

Fig. 8 Bright-field TEM image of alloy with 0.5% C aged at 800 °C for 75 h in needle-liked carbides (a), fine $\beta/B2$ grains and corresponding selected-area electron diffraction (SAED) pattern (b)

4 Conclusions

1) The proportion of β phase is affected by the content of carbon. With the increase of carbon addition, the content of β phase in the alloy decreases obviously, but the colony size increases.

2) Carbon atom can decrease the lamellar spacing, while an excess of carbon may increase the lamellar spacing due to coarse carbon precipitates.

3) Among these four alloys, Ti−45Al−3Fe−2Mo−0.5C exhibits homogeneous microstructure with fine lamellar spacing and large colony size, which can assure optimum high temperature properties, especially high-temperature creep property.

4) P-type carbides grow up with prolonging aging time at the boundaries and near the dislocation areas at temperature of 800 °C. More and coarser precipitates are found with extending treating time.

References

[1] KIM Y W, DIMIDUK D M. Progress in the understanding of gamma titanium aluminide [J]. JOM, 1991(8): 40−47.

[2] WU Xin-hua. Review of alloy and process development of TiAl alloys [J]. Intermetallics, 2006, 14: 1114−1122.

[3] KIM Y W, MORRIS D, YANG R, LEYENS C. Structural aluminides for elevated temperature applications [M]. Warrendale: Wiley, 2008.

[4] YAMAGUCHI M, INUI H, KISHIDA K, MATSUMORO M, SHIRAI Y. Gamma titanium aluminide alloys [M]. Cambridge: Cambridge University Press, 1994.

[5] LORETTO M H, GODFREY A B, HU D, BLENKINSOP P A, JONES I P, CHENG T T. The influence of composition and processing on the structure and properties of TiAl-based alloys [J]. Intermetallics, 1998, 6: 663−666.

[6] LIU C T, MAZIASZ P J. Microstructural control and mechanical properties of dual-phase TiAl alloys [J]. Intermetallics, 1998, 6: 653−661.

[7] CHAUDHARI G P, ACOFF V L. Titanium aluminide sheets made using roll bonding and reaction annealing [J]. Intermetallics, 2010, 18: 472−478.

[8] QIU Cong-zhang, LIU Yong, ZHANG Wei, LIU Bing, LIANG Xiao-peng. Development of a Nb-free TiAl-based intermetallics with a low-temperature superplasticity [J]. Intermetallics, 2012, 27: 46−51.

[9] QIU Cong-zhang, LIU Yong, HUANG Lan, ZHANG Wei, LIU Bing, LU Bin. Effect of Fe and Mo additions on microstructure and mechanical properties of TiAl intermetallics [J]. Transactions of Nonferrous Metals Society of China, 2012, 22: 521−527.

[10] WANG J G, NIEH T G. Creep of a beta phase-containing TiAl alloy [J]. Intermetallics, 2000, 8: 737−748.

[11] KIM Y W. Intermetallic alloys based on gamma titanium aluminide [J]. JOM, 1989, 41: 24−30.

[12] TIAN W H, NEMOTO M. Effect of carbon addition on the microstructures and mechanical properties of γ-TiAl alloys [J]. Intermetallics, 1997, 5: 237−244.

[13] PERDRIX F, TRICHET M F, BONNENTIEN J L, CORNET M, BIGOT J. Influence of nitrogen on the microstructure and mechanical properties of Ti−48Al alloy [J]. Intermetallics, 2001, 9: 147−155.

[14] MENAND A, HUGUET A, NÉRAC-PARTAIX A. Interstitial solubility in γ and α_2 phases of TiAl-based alloys [J]. Acta Materialia, 1996, 44: 4729−4737.

[15] PERDRIX F, TRICHET M F, BONNENTIEN J L, CORNET M, BIGOT J. Relationships between interstitial content, microstructure and mechanical properties in fully lamellar Ti−48Al alloys, with special reference to carbon [J]. Intermetallics, 2001, 9: 807−815.

[16] PARK H S, NAM S W, KIM N J, HWANG S K. Refinement of the lamellar structure in TiAl-based intermetallic compound by addition of carbon [J]. Scripta Materialia, 1999, 41: 1197−1203.

[17] CHRISTOPH U, APPEL F, WAGNER R. Dislocation dynamics in carbon-doped titanium aluminide alloys [J]. Materials Science and Engineering A, 1997, 239−240: 39−45.

[18] GERLING R, SCHIMANSKY F P, STARK A, BARTELS A, KESTLER H, CHA L, SCHEU C, CLEMENS H. Microstructure and mechanical properties of Ti45Al5Nb(0−0.5C) sheets [J]. Intermetallics, 2008,16: 689−697.

[19] SCHEU C, STERGAR E, SCHOBER M, CHA L, CLEMENS H, BARTELS A, SCHIMANSKY F P, CEREZO A. High carbon solubility in a γ-TiAl-based Ti−45Al−5Nb−0.5C alloy and its effect on hardening [J]. Acta Materialia, 2009, 57: 1504−1511.

[20] CHEN Yu-yong, NIU Hong-zhi, KONG Fan-tao, XIAO Shu-long. Microstructure and fracture toughness of a β phase containing TiAl alloy [J]. Intermetallics, 2011,19: 1405−1410.

[21] DENQUIN A, NAKA S. Phase transformation mechanisms involved in two-phase TiAl-based alloys—I. Lambellar structure formation [J]. Acta Materialia, 1996, 44: 343−352.

C 元素对 Ti−45Al−3Fe−2Mo−*x*C 合金显微组织的影响

周灿旭，刘 彬，刘 咏，邱从章，贺跃辉

中南大学 粉末冶金国家重点实验室，长沙 410083

摘 要：研究 C 元素对 TiAl 基合金(Ti−45Al−3Fe−2Mo)显微组织的影响。随着 C 元素含量的增加，合金中 β 相含量的比例降低，而片层晶团尺寸增大。当 C 含量增加至 0.3%和 0.5%时，片层间距从 267 nm 降低至 237 nm 和 155 nm，但是进一步增加 C 含量，片层间距长大至 230 nm。这是由 C 原子的抑制作用及碳化物的析出引起的。800 °C 时效可以使 P-型碳化物析出。随着时效时间的延长，该碳化物主要在晶界处及位错线附近析出并长大，并在不同的入射角(TEM)下有不同的形貌。对其显微组织的变化进行了详细的分析及探讨。

关键词：β-TiAl 合金；碳掺杂；组织；碳化物

(Edited by Hua YANG)